Bioresource Technology 338 (2021) 125535

Contents lists available at ScienceDirect

Bioresource Technology

journal homepage: www.elsevier.com/locate/biortech

Fast-growing Paulownia wood fractionation by microwave-assisted hydrothermal treatment: A kinetic assessment

Pablo G. del Río, Beatriz Gullón, Aloia Romaní, Gil Garrote *

Universidade de Vigo, Departamento de Enxeñaría Química, Facultade de Ciencias, 32004 Ourense, Spain

HIGHLIGHTS

- Aqueous processing assisted by MW heating was proposed for PW fractionation.
- MHT is regarded as suitable approach for advancing second-generation biorefineries.
- MW provoked a solubilization of Xn of up to 1.6-fold higher compared to CHT.
- Kinetic models used can be proper to predict other biomasses' behaviors after MHT.
- 13.9 g of XO per 100 g of PW were obtained by MHT (80% recovery of initial xylan).

GRAPHICAL ABSTRACT

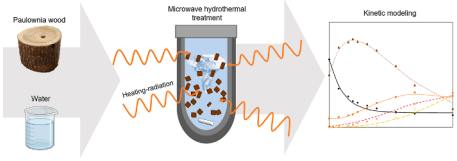

ARTICLE INFO

Keywords:
Paulownia
Biorefinery
Microwave
Autohydrolysis
Kinetics
Oligomers

ABSTRACT

Microwave hydrothermal treatment (MHT), a novel advanced technology, was proposed for the fractionation of Paulownia wood (PW) at temperatures ranging 200–230 °C and residence times of 0–50 min, corresponding to severities of 2.93–4.70. This procedure allowed 80% of xylan recovery as xylooligosaccharides and an average of 95% cellulose recovery in the pretreated PW biomass, showing the selectivity of the treatment, that was also compared to conduction–convection heating autohydrolysis. Finally, a kinetic model was proposed for the prediction of PW fractionation using MHT, with the ultimate goal of being applied to a wide range of feedstocks and minimizing the number of parameters used. For that, two strategies were approached, allowing the reduction of 80 to 34 parameters, without significant influence in the kinetic fitting. To the best of our knowledge, this is the first kinetic modelization of MHT of PW, taking into account all the lignocellulosic fractions.

Abbreviations: AcG, acetyl groups); AcH, acetic acid); AcO, acetyl groups linked to oligosaccharides); Ar, arabinose); Arn, arabinan); ArO, arabinooligosaccharides; CHT, conduction–convection hydrothermal treatment; DP, degradation products; Ea, activation energy; F, furfural; G, glucose; GHGs, Green House Gases; Gn, glucan; GO, glucooligosaccharides; HMF, 5-Hydroxymetyl-2-furfural; HPLC, High Performance Liquid Chromatography; IR, infrared; KL, Klason lignin; LCB, lignocellulosic biomass; MW, microwave; MHT, microwave hydrothermal treatment; NVC, non-volatile compounds; PW, Paulownia wood; QAH, Quantitative Acid Hydrolysis; RM, Raw material; S_0, severity; T, temperature; t, time; TS, total solids; VC, volatile compounds; X, xylose; Xn, xylan; XO, xylooligosaccharides; XO_H, high molecular weight xylooligosaccharides; XO_L, low molecular weight xylooligosaccharides..

* Corresponding author.
E-mail address: gil@uvigo.es (G. Garrote).

https://doi.org/10.1016/j.biortech.2021.125535
Received 7 June 2021; Received in revised form 6 July 2021; Accepted 7 July 2021
Available online 17 July 2021

1. Introduction

Currently, the increase of population and environmental issues due to carbon and greenhouse gas emissions (GHGs) has raised the interest in the employment of green and renewable resources to substitute oil refineries. Consequently, the biorefineries are systems that deal with the manufacture of bio-based products, such as chemicals and fuels, transforming a biological feedstock (biomass) by different procedures (Cao et al., 2020; Fernandes Antunes et al., 2019; Jorissen et al., 2020).

This is the case of second generation biorefineries, where lignocellulosic biomass (LCB) is utilized as feedstock. In this context, the use of LCB is interesting because it comprises non-edible materials for instance wood, industrial or agricultural wastes and energy crops (Chandel et al., 2020; Oleszek et al., 2019) that exhibits some benefits such as being ubiquitous, renewable, sustainable, and having high production capacity and low cost (Ferreira and Taherzadeh, 2020; Ingle et al., 2020). Specifically, energy crops have a remarkable versatility and are very appropriate for biorefinery purposes due to their high biomass yield and content of valuable constituents for the pharmaceutical, food, chemical or energy sectors (Oleszek et al., 2019). In this context, Paulownia is a fast growing tree with a high biomass production (up to 50 t/(ha·year)) which can be employed as an energy crop due to its growth rate and low necessity of water (del Río et al., 2020a).

Moreover, LCB has a complex structure mainly made up of cellulose, hemicelluloses and lignin. In order to obtain a wide range of bio-based products and bioenergy, the fractionation of the LCB into its main components plays a key role (del Río et al., 2020c; Sanahuja-Parejo et al., 2019). Hydrothermal treatment (also known as autohydrolysis) is a promising pretreatment that employs high temperature and water as an only reagent to hydrolyze the LCB (del Río et al., 2019; Domínguez et al., 2017). The combination of both, temperature and water, provokes the self-ionization of water and the consequent solubilization of hemicelluloses (Vargas et al., 2016). Suitable conditions of operation may lead to maximum release of hemicellulosic-derived compounds, mostly in the form of xylooligosaccharides, which have prebiotic activity (Dávila et al., 2019) and can also be employed, for instance, to produce other compounds such as lipids for the nutraceutical industry (Díaz-Fernández et al., 2019), biofuels for the energy industry (Cunha et al., 2019; Domínguez et al., 2021) or xylitol for the food industry (Romaní et al., 2020). On the other hand, the remaining solid fraction is essentially composed by cellulose and lignin and exhibits good enzymatic susceptibility to produce glucose, which can be converted into important manufactured products such as bioethanol (Vargas et al., 2016), bio-succinic acid (González-García et al., 2018), lactic acid (Gullón et al., 2020), or hydroxymethylfurfural (Sweygers et al., 2020), among others.

Besides the conventional heating reactors, a novel advanced technology such as microwave (MW) is considered a greener procedure that can enable a faster and more effective heating, with a consequent reduction of energy (Aguilar-Reynosa et al., 2017a, 2017b; Chin et al., 2014; Ershova et al., 2015). On the one hand, a conventional heating transmits the heat from the outside to the inside, leading to a loss of energy in the transmission from the heating generator through the vessel or recipient until the to-be-pretreated biomass. In addition, the formation of overheated or cooler regions inside the reactor is more than likely. Nevertheless, if microwave technology is used, the heat is uniformly and directly transmitted to the biomass, because it is induced at a molecular level due to the direct conversion of the electromagnetic energy into heat (López-Linares et al., 2019). Thus, this method is highly selective and facilitates a homogeneous heating because the radiation is only absorbed by the solvent or biomass (Aguilar-Reynosa et al., 2017a; del Río et al., 2020b). In this context, microwave hydrothermal treatment (MHT) combines the advantages of water-based treatments, with the beneficial effect of microwave, providing a fast and effective heating over the biomass (Meng et al., 2016; Zhu and Chen, 2014).

In order to favor the comprehension of the hydrolytic phenomena over the biomass, which is essential for the optimization, design and scale-up of the process, accurate kinetic models have to be developed (being simple and easily understandable). These models allow the prediction of the optimal conditions for the biomass fractionation, such as solubilization of high-added value hemicelluloses (Gullón et al., 2017), or changes over the cellulose (dos Santos Rocha et al., 2017).

In this context, the kinetic models exhibit two main advantages, such as: (i) facilitating the understanding of the process phenomenology by the analysis of the behavior of the different fractions studied and their relationship, and (ii) supplying equations that allow to calculate the concentration of the involved species at different temperatures and times. In addition, these equations can be employed for techno-economic optimization studies. In fact, kinetic models have been mainly developed for the evaluation of hemicelluloses solubilization using hydrothermal treatment from several raw materials namely, *Acacia dealbata* (Yáñez et al., 2009), vine shoots (Gullón et al., 2017), *Annona cherimola* Mill. seeds (Branco et al., 2015), sugarcane bagasse (Santucci et al., 2015), inter alia.

In this sense, the great majority of these kinetic models are grounded on the modelization of the hydrolysis of xylan (Santucci et al., 2015) or hemicelluloses (Gullón et al., 2017), since they belong to the most affected fraction in this kind of pretreatments. The purpose of this work is the modelization of every fraction affected by the microwave pretreatment, in order to achieve a better understanding of the process. There are some works that dealt with the use of microwave to pretreat the biomass using sulfuric acid hydrolysis (Chin et al., 2014), or to produce furans using ionic liquids (da Silva Lacerda et al., 2015) or biphasic reactions (Sweygers et al., 2020). However, to the best of our knowledge, the kinetic modeling of microwave-assisted autohydrolysis is still unexplored in the scientific literature.

In this way, the aim of this work was the optimal fractionation of Paulownia wood using microwave hydrothermal treatment assessed via kinetic models. To this end, in depth evaluation of microwave hydrothermal treatment was assessed using four different temperatures (200, 210, 220 and 230 °C) at different residence times (0–50 min), taking into account the severity of the process. Carbohydrates analysis of the solid and liquid fractions, solid yield, non-volatile compounds and volatile compounds were determined. Afterwards, data were subjected to a kinetic model for a better optimization of the process, where all the species (glucan, xylan, arabinan, acetyl groups and total solids) were evaluated. As far as the authors know, no other research dealt with the kinetic modelization of microwave assisted autohydrolysis of all the fractions with Paulownia wood.

2. Materials and methods

2.1. Feedstock and chemical composition

Paulownia elongata × *fortunei* wood was employed as feedstock for this research, and it was kindly provided by a local company (Maderas Álvarez Oroza S. L., NW Spain). After bark removal, Paulownia wood (PW) was air-dried, milled and sieved to obtain a homogeneous lot with a particle size smaller than 1 mm.

Subsequently, PW was chemically determined employing NREL analytical procedures for ashes (Sluiter et al., 2008b), extractives (Sluiter et al., 2008d), moisture (Sluiter et al., 2008a) and quantitative acid hydrolysis (QAH) (Sluiter et al., 2008c). All the assays were performed in triplicate. Solid phase after QAH (namely acid insoluble residue) was weighted and identified as Klason lignin (KL). Liquid phase after QAH was employed for analysis via high performance liquid chromatography (HPLC) for monosaccharides (glucose, xylose, and arabinose) and acetic acid concentration in order to determine the content of glucan, xylan, arabinan and acetyl groups (employing a Phenomenex Rezex ROA-Organic Acid H^+ (8%) column at 60 °C and 0.6 mL/min of flow rate with 3 mM H_2SO_4 mobile phase and a refractive index detector at 40 °C).

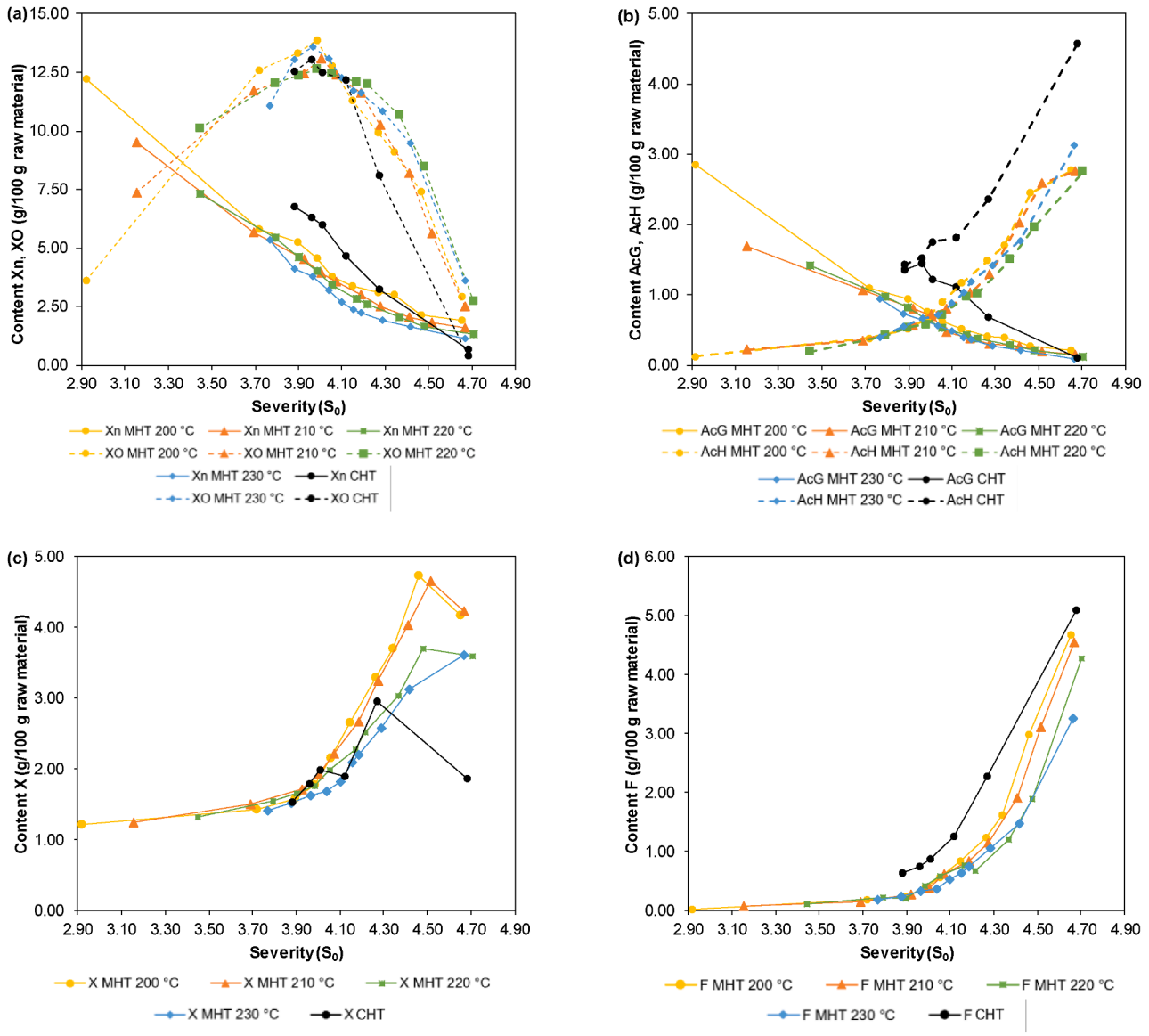

Fig. 1. Profiles of (a) Xn -xylan-, XO -xylooligosaccharides-, (b) AcG -acetyl groups-, AcH -acetic acid-, (c) X -xylose-, and (d) F -furfural- regarding the severity for microwave hydrothermal treatment -MHT- at 200, 210, 220 and 230 °C in comparison with conduction–convection hydrothermal treatment -CHT-. Data from CHT extracted from del Río et al. (2020) (del Río et al., 2020a).

The chemical composition of *Paulownia elongata* × *fortunei*, measured as g of component/100 g PW, based on triplicates, was as follows: glucan 42.2 ± 0.13, xylan 17.3 ± 0.03, arabinan 0.84 ± 0.01, acetyl groups 3.76 ± 0.03, Klason lignin 20.7 ± 0.15, extractives 5.21 ± 0.00, ashes 0.53 ± 0.00.

2.2. Microwave hydrothermal treatment (MHT)

A blend of PW and water, at a consistency (C) of 6 g of PW/100 g of total weight, was employed in the microwave hydrothermal treatment (MHT). Experiments were carried out in a Monowave 450 single-mode microwave reactor (Anton Paar GmbH) equipped with an air compressor to cool the sample. Heating time was set at 5 min for all the assays, temperature was measured by the IR detector, stirring speed was set at 900 rpm, and the cooling time varied between 5 and 6 min. The reactions were performed in standard 30 mL Pyrex vessel (G30).

PW was subjected to MHT at 4 different temperatures and 10 different residence times for each temperature: 200 °C from 0 to 50 min, 210 °C from 0 to 26 min, 220 °C from 0 to 14 min and 230 °C from 0 to 6 min (40 treatment experiments).

2.3. Chemical analysis of microwave pretreated PW

After the MHT was performed at desired temperature and retention time, the whole slurry was filtrated, separating the liquid (liquor) and solid fractions. The solid phase was subsequently washed with distilled water until neutral pH, weighted for solid yield determination and analyzed via QAH as described in section 2.1. The liquor was divided in three aliquots (as explained by (del Río et al., 2020c)) for: (i) non-volatile compounds determination, (ii) direct analysis of the liquor via HPLC, and (iii) acid posthydrolysis 4% w/w H_2SO_4 at 121 °C for 20 min for HPLC analysis. Experiments were performed in triplicate.

2.4. Data fitting

The experimental results were fitted to the proposed kinetic models via a minimization of the sum of squares employing a commercial software with a built-in optimization routine grounded on Newton's

method (Solver, Microsoft Excel).

3. Results and discussion

3.1. Microwave hydrothermal treatment of Paulownia wood: experimental data of liquid and solid phases characterization

After the microwave processing, resulting solid and liquid fractions were chemically analyzed, comprising data about process fractionation (solid yield, non-volatile compounds, volatile solid content), and chemical composition of the solid and liquid fractions (measured in g component/100 g of raw material).

In order to make a better comparison within the different experiments, temperature and time (including time of heating, treatment and cooling) were employed to calculate the harshness of the process, that is expressed with the severity (S_0) as follows:

$$S_0 = \log R_0 = \log(R_{0HEATING} + R_{0ISOTHERMAL} + R_{0COOLING}) = \quad (1)$$

$$= \log\left(\int_0^{t_H} \exp\cdot\left(\frac{T(t) - T_{REF}}{\omega}\right)\cdot dt + \exp\cdot\left(\frac{T_{ISOT} - T_{REF}}{\omega}\right)\cdot t_{ISOT} + \int_{t_H + t_{ISOT}}^{t_H + t_{ISOT} + t_C} \exp\cdot\left(\frac{T'(t) - T_{REF}}{\omega}\right)\cdot dt \right)$$

where R_0 represents the severity factor, T(t) and T'(t) are the temperature profiles in the heating and cooling stages respectively, t_H (min) is the time which is necessary to reach the target temperature T_{ISOT} (°C), the temperature which is employed in the isothermal processing for a time t_{ISOT} (min), t_C (min) is the time employed in the cooling period, ω is the empiric parameter related to activation energy and T_{REF} is the temperature of reference (commonly values: ω = 14.75 °C and T_{REF} = 100 °C).

Firstly, the solid yield reflected the effect of the treatment on the material. Consequently, it decreased when the severity of the treatment augmented, ranging values of 65.4–87.3 g of solid phase/100 g of raw PW. Furthermore, if comparing these values with the sum of glucan and lignin in the raw material (62.9 g /100 g of raw PW), it may reflect that these two fractions may be scarcely affected by the pretreatment, even at higher severities. On the other hand, non-volatile compounds (NVC) and volatile compounds (VC) (which sum represent the solubilization degree) varied among values of 13.7–27.4 and 0.00–16.8 g/100 g of raw PW, respectively. Maximum values of NVC were observed at severities close to 4.00, which corresponded to the maximum release of oligomers in the liquid phase, whereas the VC increased its value with the time owing to the production of volatile compounds such as acetic acid or furfural.

Concerning the solid composition, glucan was the major component in the solid, presenting scarcely variation (38.4–41.3 g of glucan/100 g of raw PW), maintained in an average of 95% of recovery regarding the initial glucan at any temperature. The second major component in the solid was the lignin, with recovery values close or slightly superior to 100%, that can be as a result of its bonding with products from the solubilization and/or degradation of polysaccharides, with lignin degradation products or due to the quantification of extracts as pseudolignin (Sannigrahi et al., 2011) as previously happened when employing conventional-heating autohydrolysis of Paulownia wood (del Río et al., 2020a; Domínguez et al., 2020). In contrast, the courses for hemicelluloses (xylan, arabinan and acetyl groups) were similar, presenting a higher solubilization compared to glucan.

On the subject of the liquid phase composition, it was majorly composed by oligosaccharides, especially xylooligosaccharides (XO) which maximum content was in a severity of 3.97–4.00, reaching 12.6–13.9 g of XO/100 g of raw PW, meaning a recovery of 72.8–80.1% regarding initial xylan (Xn). At harsher conditions, the XO decreased triggering xylose (X) formation, and subsequently furfural until maximum values of 3.26–4.67 g of furfural/100 g raw material at the highest severity (4.65–4.70). In the case of the sum of XO + X, maximum contents of 14.4–15.7 g of XO + X/100 g of raw PW were obtained, meaning a recovery among 83.0–90.4% regarding initial xylan, reached at the same severity as for the maximum recovery of XO (S_0 of 3.97–4.00). Similar behaviors were noticed for the other species of hemicelluloses present in the PW (related to arabinan and acetyl groups).

3.2. Comparison of microwave and conventional heating systems for hydrothermal treatment of PW

The expression of fractionation data as function of the severity allows an easy interpretation of the results obtained in this work, as well as a better comparison with other heating treatments such as conduction–convection. Taking into account that the radiation may perform an additional effect on the biomass' pretreatment, results obtained in this work were compared to those from conduction-convection hydrothermal treatment (CHT) (known as autohydrolysis) of PW, previously reported by our group (del Río et al., 2020a). Fig. 1 represents the variation of the xylan (Xn), xylooligosaccharides (XO), acetyl groups (AcG), acetic acid (AcH), xylose (X) and furfural (F) as a function of the severity of the different hydrothermal treatments.

When comparing MHT and CHT, similar dynamics could be observed although there were some nuances to take into account. On the one hand, the glucan content was very similar no matter the pretreatment employed, nevertheless at severities ≥ 4.12, there was a minor loss of glucan in the solid phase after CHT, with a recovery of 88.3% of glucan regarding the initial glucan (del Río et al., 2020a), compared to MHT with 90.8–93.5% of glucan recovery regarding the initial glucan. Contrariwise, Klason lignin content was higher after CHT, in the order of 26.2–28.3 g of lignin/100 g of raw PW (del Río et al., 2020a), whereas after MHT was about 20.3–24.0 g of lignin/100 g of raw PW, which indicates that the conventional-heating may affect considerably the adhesion of carbohydrates, extracts and other compounds to the lignin, incrementing its final value.

On the other hand, the use of MW affected the solubilization of compounds to a larger extent, as can be seen in Fig. 1a for xylan and 1b for acetyl groups. Those graphics reflect a lower solubilization when using CHT if compared with MW at the same severities. For instance, at severity of 3.88–3.92, MW provoked a solubilization of 1.3–1.6 and 1.5–1.9-fold higher for Xn and AcG, respectively, if compared with CHT (del Río et al., 2020a). This may be owing to the kind of heating, i.e., the conduction–convection heating, that may lead to a different way of depolymerization and solubilization of compounds. However, at the highest severity studied (4.65–4.70), the Xn and AcG content of the solid phase was reasonably similar no matter the use of MHT or CHT.

Alternatively, although the amount of oligosaccharides was similar, for example the maximum of XO at S_0 of 3.97–4.00, with values of 12.6–13.9 g of XO/100 g raw PW after MW and 13.1 g XO/100 g raw PW after CHT, it can be highlighted that the MW processing enabled a slight improve in the release of XO, besides presenting a lower depolymerization of XO compared with the use of conventional heating (see Fig. 1a). Higher XO production from corn stover using MW in comparison with conduction–convection heating was also reported in the literature (Aguilar-Reynosa et al., 2017b). Similarly, xylose (consult Fig. 1c) content in CHT was maintained in the range of MHT, however in the highest severity (4.65–4.70), the value was drastically reduced to 1.86 g of xylose/100 g of raw PW, in comparison with MW values of 3.61–4.24 g xylose/100 g of raw PW. Acetic acid (AcH) and furfural (F) profiles are displayed in Fig. 1b and 1d. In these cases, higher amounts of AcH and F were obtained when carrying out autohydrolysis via conventional heating in comparison with MHT, regardless the severities compared, reaching, at the highest severity (4.65–4.70) 1.5–1.7, and 1.1–1.6-fold higher for AcH and F, respectively. As in the prior case, this behavior may be due to the kind of heating, that provokes a different profile of depolymerization. A comparable situation was reflected in the

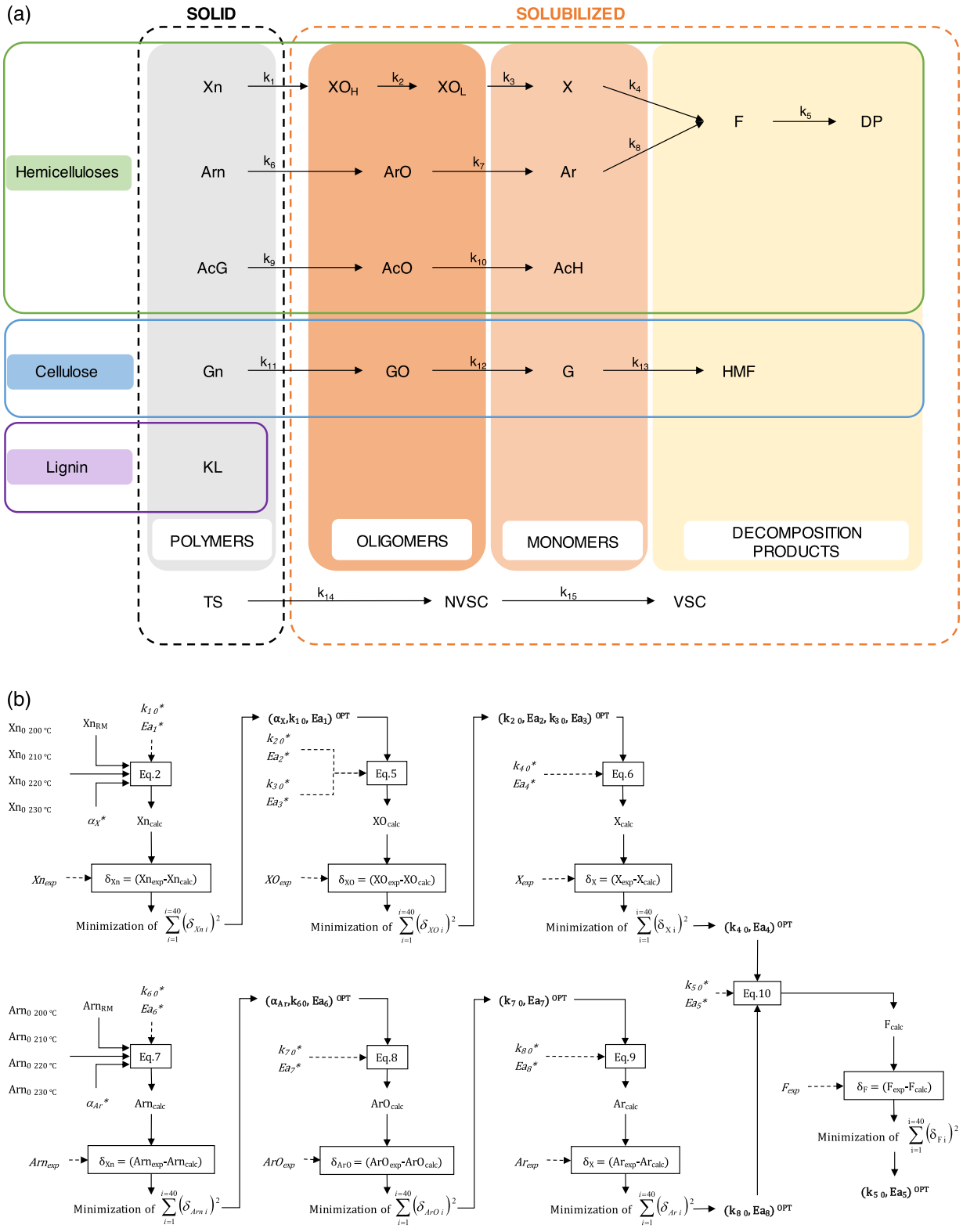

Fig. 2. (a) Kinetic model for the microwave-assisted autohydrolysis of *Paulownia elongata* × *fortunei* wood and (b) algorithm for the determination of the optimal values of kinetic parameters for xylan and arabinan fractions.

case of hydroxymethylfurfural (HMF) at the highest severity, besides the fact that glucan was more depolymerized after CHT so it can be easily transformed in HMF, whereas MW barely affected the stability of glucan and the HMF content was much lower.

In this context, the main compelling reason that may influence the behavior of these species was the difference between conduction–convection heating employed in CHT, compared to the use of microwave radiation in MHT, that may enhance the pretreatment not only by the use of heat but due to the vibration energy that affects the molecules of the LCB (Aguilar-Reynosa et al., 2017a).

Table 1
Values of (i) the susceptible fraction (α) for xylan (Xn), arabinan (Ar), acetyl groups (AcG), glucan (Gn) and total solids (TS), (ii) kinetic coefficients from k1 to k15 (see Fig. 2 for coefficients definition) and, (iii) coefficient of determination R^2 after MHT of PW.

	Temperature (°C)			
	200	210	220	230
α_{Xn}	0.849	0.887	0.916	0.919
α_{Arn}	0.943	0.963	0.971	0.979
α_{AcG}	0.904	0.937	0.944	0.971
α_{Gn}	0.0091	0.0145	0.0244	0.0193
α_{TS}	0.328	0.326	0.340	0.348
k_1 (min^{-1})	0.232	0.309	0.414	1.138
k_2 (min^{-1})	0.0571	0.120	0.202	0.464
k_3 (min^{-1})	0.0571	0.120	0.203	0.464
k_4 (min^{-1})	0.0413	0.0915	0.196	0.477
k_5 (min^{-1})	0.0245	0.0746	0.167	0.565
k_6 (min^{-1})	0.200	0.246	0.421	0.941
k_7 (min^{-1})	0.0176	0.0264	0.0339	0.0875
k_8 (min^{-1})	0.0517	0.108	0.181	0.409
k_9 (min^{-1})	0.234	0.346	0.511	0.876
k_{10} (min^{-1})	0.0357	0.0567	0.117	0.876
k_{11} (min^{-1})	0.151	0.233	0.351	0.534
k_{12} (min^{-1})	0.0101	0.0320	0.0647	0.121
k_{13} (min^{-1})	0.0111	0.0446	0.117	0.235
k_{14} (min^{-1})	0.154	0.203	0.453	0.560
k_{15} (min^{-1})	0.0131	0.0234	0.0533	0.0958
R^2 of Xn	0.988	0.990	0.998	0.981
R^2 of XO	0.989	0.984	0.962	0.987
R^2 of X	0.983	0.995	0.968	0.955
R^2 of F	0.985	0.966	0.928	0.950
R^2 of Arn	0.9999	0.9999	0.9999	0.9999
R^2 of ArO	< 0.8	< 0.8	< 0.8	< 0.8
R^2 of Ar	< 0.8	< 0.8	< 0.8	< 0.8
R^2 of AcG	0.992	0.988	0.987	0.987
R^2 of ArO	0.978	0.882	0.960	0.960
R^2 of Gn	< 0.8	< 0.8	< 0.8	< 0.8
R^2 of GO	0.852	0.860	0.871	< 0.8
R^2 of G	0.953	0.910	0.947	0.933
R^2 of TS	0.989	0.977	0.987	0.933
R^2 of NVC	0.961	0.908	0.952	0.924

Table 2
Kinetic coefficient fitting with the Arrhenius equation.

k_i (min^{-1})	ln k_{0i} (k_{0i} in min^{-1})	Ea (kJ/mol)	R^2
k_1 (min^{-1}) Xn → XO_H	23.7	99.7	0.881
k_2 (min^{-1}) XO_H → XO_L	31.4	135	0.992
k_3 (min^{-1}) XO_L → X	31.4	135	0.992
k_4 (min^{-1}) X → F	37.5	160	0.998
k_5 (min^{-1}) F → DP	47.7	202	0.993
k_6 (min^{-1}) Arn → ArO	24.2	102	0.929
k_7 (min^{-1}) ArO → Ar	21.2	99.7	0.912
k_8 (min^{-1}) Ar → F	30.9	133	0.992
k_9 (min^{-1}) AcG → AcO	20.3	85.9	0.990
k_{10} (min^{-1}) AcO → AcH	47.9	203	0.880
k_{11} (min^{-1}) Gn → GO	19.2	83.1	0.9998
k_{12} (min^{-1}) GO → G	36.6	162	0.982
k_{13} (min^{-1}) G → HMF	46.7	201	0.982
k_{14} (min^{-1}) TS → NVC	21.6	92.4	0.945
k_{15} (min^{-1}) NVC → VC	29.8	134	0.994

3.3. Kinetic model using pseudo-homogeneous reactions

Two premises are essential to establish a kinetic model: (i) the requirement of obtaining the more detailed information, i.e. the seek for a model that explains the behavior of as many species as possible, and (ii) once the model explains satisfactorily the process, it must be as simple as possible, minimizing the number of parameters to be determined. In this context, the fact that all the kinetic reactions involved are irreversible, first-order and pseudohomogeneous was considered (Caparrós et al., 2006).

Table 3
Results of the fitting after modeling all the temperatures jointly: (i) susceptible fraction, (ii) ln of the kinetic coefficients (ln k_{0i}), activation energy (Ea) and (iii) coefficient of determination R^2 for each species and each temperature.

Susceptible fraction (g/g)				
α_{Xn}	0.888			
α_{Arn}	1			
α_{AcG}	0.933			
α_{Gn}	0.0550			
α_{TS}	0.335			
	ln k_{0i} (k_{0i} in min^{-1})		Ea (kJ/mol)	
k_1 (min^{-1}) Xn → XO_H	29.8		124	
k_2 (min^{-1}) XO_H → XO_L	29.6		128	
k_3 (min^{-1}) XO_L → X	27.6		119	
k_4 (min^{-1}) X → F	33.4		144	
k_5 (min^{-1}) F → DP	40.1		171	
k_6 (min^{-1}) Arn → ArO	20.1		86.4	
k_7 (min^{-1}) ArO → Ar	28.5		129	
k_8 (min^{-1}) Ar → F	32.3		139	
k_9 (min^{-1}) AcG → AcO	25.9		108	
k_{10} (min^{-1}) AcO → AcH	25.0		111	
k_{11} (min^{-1}) Gn → GO	20.4		87.3	
k_{12} (min^{-1}) GO → G	13.6		69.8	
k_{13} (min^{-1}) G → HMF	44.0		192	
k_{14} (min^{-1}) TS → NVC	19.2		83.1	
k_{15} (min^{-1}) NVC → VC	30.5		137	
	Temperature (°C)			
	200	210	220	230
R^2 of Xn	0.978	0.988	0.962	0.875
R^2 of XO	0.972	0.988	0.939	0.959
R^2 of X	0.988	0.990	0.964	0.932
R^2 of F	0.982	0.962	0.895	0.985
R^2 of Arn	0.9996	0.9999	0.9999	0.9999
R^2 of ArO	< 0.8	< 0.8	< 0.8	< 0.8
R^2 of Ar	< 0.8	< 0.8	< 0.8	< 0.8
R^2 of AcG	0.989	0.988	0.980	0.901
R^2 of ArO	0.961	0.854	0.974	0.951
R^2 of Gn	< 0.8	< 0.8	< 0.8	0.908
R^2 of GO	0.942	0.805	< 0.8	< 0.8
R^2 of G	0.993	0.861	0.921	0.952
R^2 of TS	0.982	0.950	0.881	< 0.8
R^2 of NVC	0.935	0.952	0.967	0.952

In previous sections, the effect of the MHT on PW fractionation was discussed, with particular attention to the solubilization of the hemicelluloses and the effect on the recovery of each fraction (namely, cellulose and lignin). From this information, conclusions of interest for the kinetic modeling are drawn. Firstly, the lignin was not especially affected by the microwave-assisted process, although increasing its value regarding the initial lignin, probably due to the decomposition products' condensation, that precipitated over the lignin. The majority of the glucan remained in the solid fraction, and the small quantity that was solubilized, was detected as little amounts of glucooligosaccharides, glucose and HMF in the liquid fraction. On the other hand, the hemicelluloses were the most affected fraction in the process, reaching an almost completely solubilization, and were present in the liquid fraction as oligomers, monomers or monomers' degradation products.

The polymers are usually considered as two-fraction compounds, i.e. being made up of a more reactive fraction (namely fast or susceptible) and a less reactive fraction (also known as slow or non-susceptible). These fractions are interrelated by the parameter α, which is the mass fraction of fast/susceptible polymer regarding the polymer. The existence of this fast/susceptible fraction is often attributed to differences in the composition of the biomass (Caparrós et al., 2006; Carvalheiro et al., 2005), whereas it is more likely to be as a result of the accessibility to the polymeric fraction which is closer and probably more bonded to the lignin.

During these processes, the polymers are solubilized in the form of oligomers, which is the most challenging fraction to be modeled,

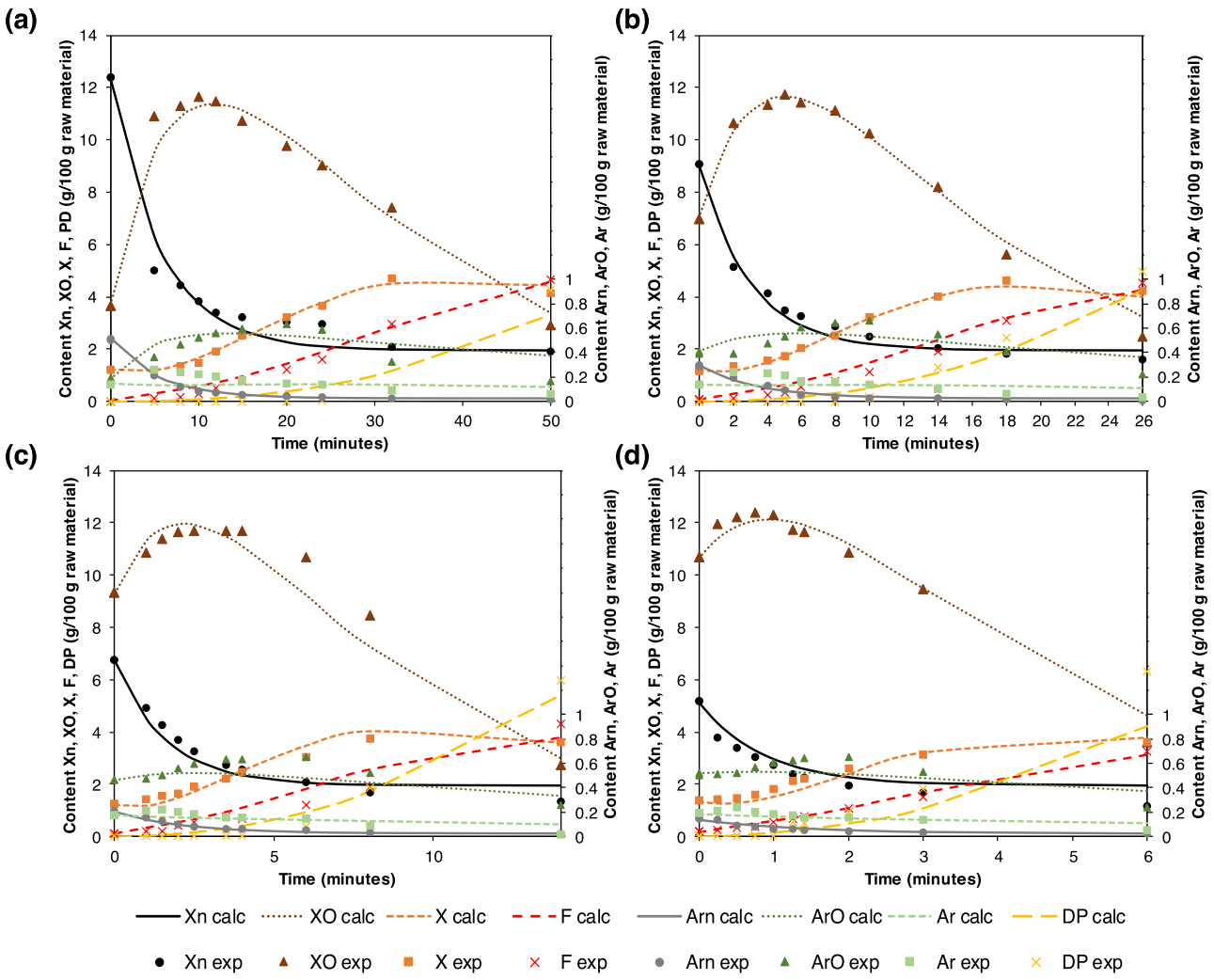

Fig. 3. Calculated (lines) and experimental (symbols) time courses for pentoses after microwave hydrothermal treatment of Paulownia wood at temperatures of (a) 200, (b) 210, (c) 220 and, (d) 230 °C.

especially in the case of hemicelluloses because: (i) their composition is relatively complex, with a structure mainly composed by units of xylose, partially substituted by acetyl groups and arabinose as side chain and, (ii) its ramified structure, which provokes the different reactivity and accessibility of each oligomer or each monomeric unit (Garrote et al., 2004; Gullón et al., 2012). Owing to this fact, a great variety of oligomers with different number and type of monomers were generated. As claimed by previous works of our research group, the existence of, at least, dozens of different oligomers have been determined (Kabel et al., 2002).

The development of a model that explains rigorously and accurately the generation and break of all the present oligomers is complex. However, it is useless when the kinetic model attempts to evaluate the evolution of the total amounts of oligomers. The easier option is the model with only one oligomeric fraction, which also implies an only parameter for the modeling of the oligomeric fraction. Nevertheless this scheme seems inadequate, adding to the fact that the kinetic models do not fit to the experimental data(Conner and Lorenz, 1986). Other options employed are depolymerization models, or models where the kinetic constant for the degradation of oligomers varies with the time (Lloyd and Wyman, 2003). The model that has been successfully developed by our research group employs two oligomeric fractions, with high and low molecular weight, that fit satisfactorily to the experimental data and implies only one additional parameter (Gullón et al., 2017, 2010; Yáñez et al., 2009).

Monomers are formed as a consequence of the oligomers breaking. In the case of hardwood, the monomers can be found in the form of pentoses, such as xylose and arabinose, and other compounds as acetyl groups. Pentoses can suffer degradation reactions, causing a dehydration of the monomer producing furfural, which can also be degraded to other decomposition products (that can be calculated by difference). In previous sections, the data reflected a higher amount of furfural at higher severities (larger residence times for each temperature). Nevertheless, the operation conditions conducing to the production of high amounts of furfural and degradation products have no practical interest in this study since are far from the conditions for the optimal recovery of a liquid phase, rich in either oligomers or oligomers and monomers.

Taken into account those elements, a kinetic modeling was developed and is displayed in Fig. 2a, under the following premises:

(i). All the species were expressed as equivalent in polymer per 100 g of raw material, on dry basis.
(ii). All the polymers are composed by two fractions, one susceptible to hydrolysis (the major part) and other non-susceptible. This estimation results in an adequate fitting and implies a reduction in the number of parameters whether comparing to the two-reactive fractions model, a fast and a slow one. Although the

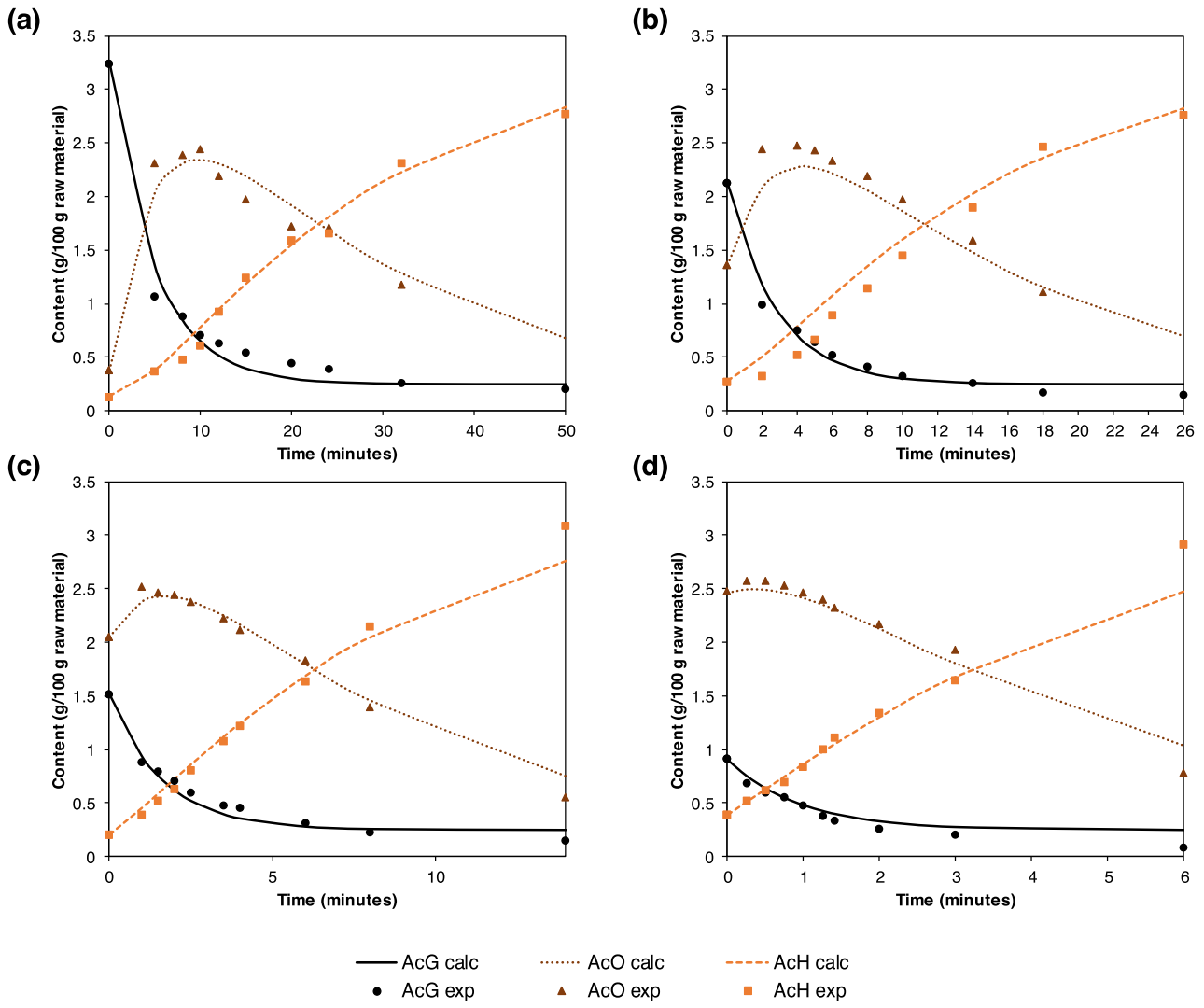

Fig. 4. Calculated (lines) and experimental (symbols) time courses for acetyl groups after microwave hydrothermal treatment of Paulownia wood at temperatures of (a) 200, (b) 210, (c) 220 and, (d) 230 °C.

modeling with two-reactive fractions has also been performed for this work (data not shown), it does not improve the fitting.

(iii). Regarding the xylan, the two-type of oligomer (high -XO_H- and low -XO_L- molecular weight) model was assumed. Regarding the rest of polymeric species, it was not necessary that model and hence, the one oligomeric fraction model fitted appropriately. This may be due to the fact that the hydrolysis of the bond that connect acetyl groups and the arabinose units to the oligomers always produce the above mentioned monomer, acetic acid and arabinose, respectively.

(iv). Concerning the glucan, it was also assumed the one oligomeric fraction model, as long as the use of the two-type of oligomer model do not provide a better fitting. Glucan led to glucose, and glucose was decomposed into HMF, which does not present decomposition to other compounds.

(v). Paying attention to the mass balances, furfural can be degraded, and the consequent reaction to the formation of degradation products (DP) was included.

(vi). In the case of acetyl groups, no decomposition phenomenon was observed from acetic acid.

(vii). Similarly, the modeling of the total solid (TS), with a susceptible and a non-susceptible fractions, was considered. This solid is solubilized into non-volatile compounds (NVC), which in turn cause the production of volatile compounds (VC).

It must be noted that, initially, all the possible reactions were considered, i.e. that the xylan fraction could be directly hydrolyzed into XO_H, XO_L, X, F, or DP; or that XO_L could be hydrolyzed either to X, F, or DP, etc. In a first modeling, all the kinetic constants were included in these reactions, adding the restriction of no negative values for the kinetic coefficients, because it was assumed that the proposed reactions were not reversible. After that, the coefficients of those 'side' reactions resulted in value of 0, reflecting that the reaction was not performed, or if it did, it was inappreciable.

The equations that regulate the kinetic modeling from Fig. 2a were as follows:

$$Xn = C_1 \cdot exp(-k_1 \cdot t) + C_2 \quad (2)$$

$$XO_H = C_3 \cdot exp(-k_1 \cdot t) + C_4 \cdot exp(-k_2 \cdot t) \quad (3)$$

$$XO_L = C_5 \cdot exp(-k_1 \cdot t) + C_6 \cdot exp(-k_2 \cdot t) + C_7 \cdot exp(-k_3 \cdot t) \quad (4)$$

$$XO = XO_H + XO_L \quad (5)$$

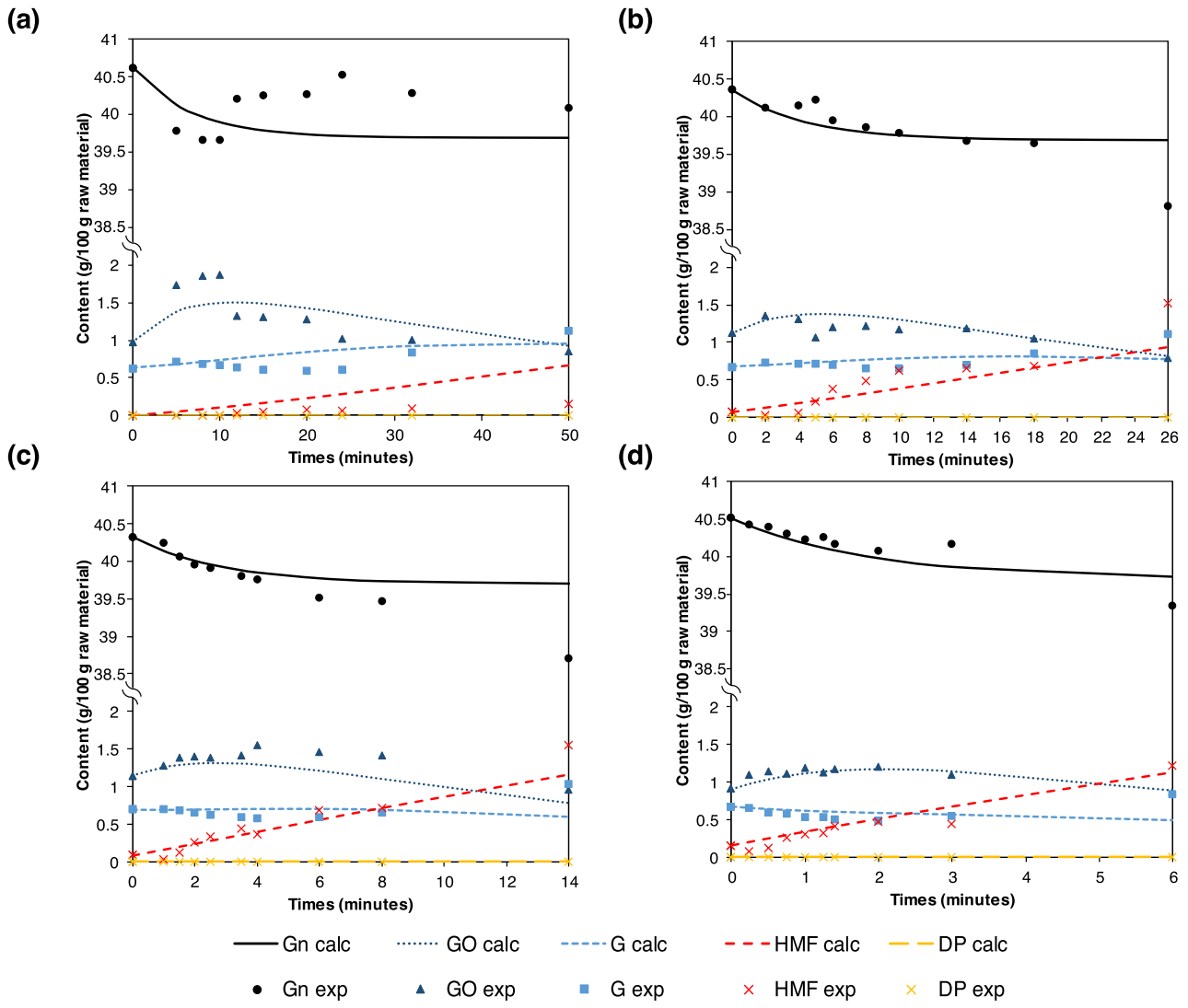

Fig. 5. Calculated (lines) and experimental (symbols) time courses for glucan after microwave hydrothermal treatment of Paulownia wood at temperatures of (a) 200, (b) 210, (c) 220 and, (d) 230 °C.

$$X = C_8 \cdot exp(-k_1 \cdot t) + C_9 \cdot exp(-k_2 \cdot t) + C_{10} \cdot exp(-k_3 \cdot t) + C_{11} \cdot exp(-k_4 \cdot t) \quad (6)$$

$$Arn = C_{12} \cdot exp(-k_6 \cdot t) + C_{13} \quad (7)$$

$$ArO = C_{14} \cdot exp(-k_6 \cdot t) + C_{15} \cdot exp(-k_7 \cdot t) \quad (8)$$

$$Ar = C_{16} \cdot exp(-k_6 \cdot t) + C_{17} \cdot exp(-k_7 \cdot t) + C_{18} \cdot exp(-k_8 \cdot t) \quad (9)$$

$$F = C_{19} \cdot exp(-k_1 \cdot t) + C_{20} \cdot exp(-k_2 \cdot t) + C_{21} \cdot exp(-k_3 \cdot t) + C_{22} \cdot exp(-k_4 \cdot t) + C_{23} \cdot exp(-k_6 \cdot t) + C_{24} \cdot exp(-k_7 \cdot t) + C_{25} \cdot exp(-k_8 \cdot t) + C_{26} \cdot exp(-k_5 \cdot t) \quad (10)$$

$$DP = Xn_{RM} + Arn_{RM} - Xn - XO_H - XO_L - X - Arn - ArO - Ar - F \quad (11)$$

$$AcG = C_{27} \cdot exp(-k_9 \cdot t) + C_{28} \quad (12)$$

$$AcO = C_{29} \cdot exp(-k_9 \cdot t) + C_{30} \cdot exp(-k_{10} \cdot t) \quad (13)$$

$$AcH = AcG_{RM} - AcG - AcO \quad (14)$$

$$Gn = C_{31} \cdot exp(-k_{11} \cdot t) + C_{32} \quad (15)$$

$$GnO = C_{33} \cdot exp(-k_{11} \cdot t) + C_{34} \cdot exp(-k_{12} \cdot t) \quad (16)$$

$$G = C_{35} \cdot exp(-k_{11} \cdot t) + C_{36} \cdot exp(-k_{12} \cdot t) + C_{37} \cdot exp(-k_{13} \cdot t) \quad (17)$$

$$HMF = Gn_{RM} - Gn - GO - G \quad (18)$$

$$TS = C_{38} \cdot exp(-k_{14} \cdot t) + C_{39} \quad (19)$$

$$NVC = C_{40} \cdot exp(-k_{14} \cdot t) + C_{41} \cdot exp(-k_{15} \cdot t) \quad (20)$$

$$VC = TS_{RM} - TS - NVC \quad (21)$$

$$C_1 = Xn_0 - Xn_{RM} \cdot (1 - \alpha_{Xn}) \quad (22)$$

$$C_2 = Xn_{RM} \cdot (1 - \alpha_{Xn}) \quad (23)$$

$$C_3 = \frac{k_1 \cdot C_1}{k_2 - k_1} \quad (24)$$

$$C_4 = XO_{H0} - C_3 \quad (25)$$

$$C_5 = \frac{k_2 \cdot C_3}{k_3 - k_1} \quad (26)$$

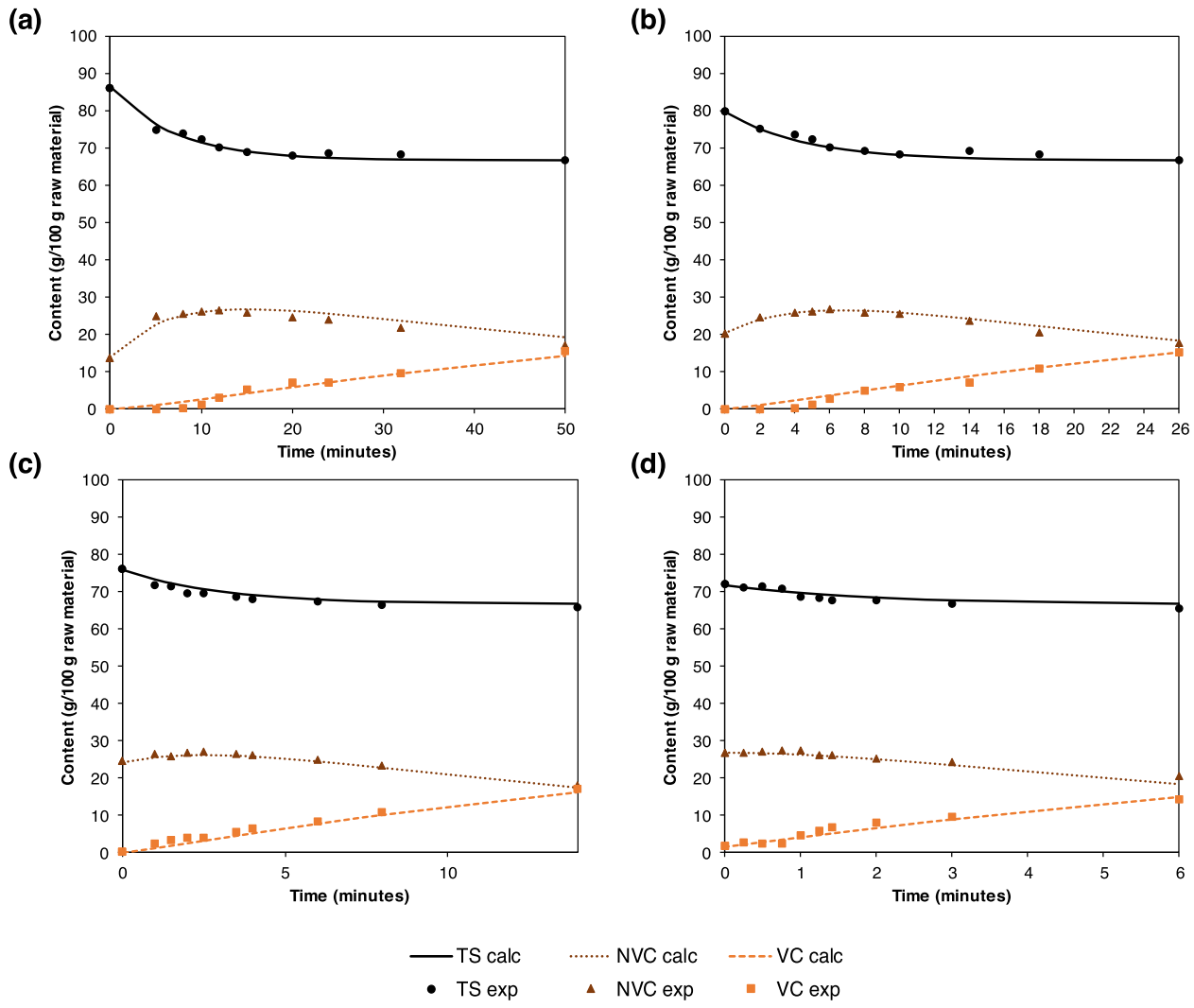

Fig. 6. Calculated (lines) and experimental (symbols) time courses for total solids after microwave hydrothermal treatment of Paulownia wood at temperatures of (a) 200, (b) 210, (c) 220 and, (d) 230 °C.

$$C_6 = \frac{k_2 \cdot C_4}{k_3 - k_2} \quad (27)$$

$$C_7 = XO_{L0} - C_5 - C_6 \quad (28)$$

$$C_8 = \frac{k_3 \cdot C_5}{k_4 - k_1} \quad (29)$$

$$C_9 = \frac{k_3 \cdot C_6}{k_4 - k_2} \quad (30)$$

$$C_{10} = \frac{k_3 \cdot C_7}{k_4 - k_3} \quad (31)$$

$$C_{11} = X_0 - C_8 - C_9 - C_{10} \quad (32)$$

$$C_{12} = Arn_0 - Arn_{RM} \cdot (1 - \alpha_{Ar}) \quad (33)$$

$$C_{13} = Arn_{RM} \cdot (1 - \alpha_{Ar}) \quad (34)$$

$$C_{14} = \frac{k_6 \cdot C_{12}}{k_7 - k_6} \quad (35)$$

$$C_{15} = ArO_0 - C_{14} \quad (36)$$

$$C_{16} = \frac{k_7 \cdot C_{14}}{k_8 - k_6} \quad (37)$$

$$C_{17} = \frac{k_7 \cdot C_{15}}{k_8 - k_7} \quad (38)$$

$$C_{18} = Ar_0 - C_{16} - C_{17} \quad (39)$$

$$C_{19} = \frac{k_4 \cdot C_8}{k_5 - k_1} \quad (40)$$

$$C_{20} = \frac{k_4 \cdot C_9}{k_5 - k_2} \quad (41)$$

$$C_{21} = \frac{k_4 \cdot C_{10}}{k_5 - k_3} \quad (42)$$

$$C_{22} = \frac{k_4 \cdot C_{11}}{k_5 - k_4} \quad (43)$$

$$C_{23} = \frac{k_8 \cdot C_{16}}{k_5 - k_6} \quad (44)$$

$$C_{24} = \frac{k_8 \cdot C_{17}}{k_5 - k_7} \quad (45)$$

$$C_{25} = \frac{k_8 \cdot C_{18}}{k_5 - k_8} \quad (46)$$

$$C_{26} = F_0 - C_{19} - C_{20} - C_{21} - C_{22} - C_{23} - C_{24} - C_{25} \quad (47)$$

$$C_{27} = AcG_0 - AcG_{RM} \cdot (1 - \alpha_{AcG}) \quad (48)$$

$$C_{28} = AcG_{RM} \cdot (1 - \alpha_{AcG}) \quad (49)$$

$$C_{29} = \frac{k_6 \cdot C_{27}}{k_7 - k_6} \quad (50)$$

$$C_{30} = AcO_0 - C_{29} \quad (51)$$

$$C_{31} = Gn_0 - Gn_{RM} \cdot (1 - \alpha_{Gn}) \quad (52)$$

$$C_{32} = Gn_{RM} \cdot (1 - \alpha_{Gn}) \quad (53)$$

$$C_{33} = \frac{k_{11} \cdot C_{32}}{k_{12} - k_{11}} \quad (54)$$

$$C_{34} = GnO_0 - C_{33} \quad (55)$$

$$C_{35} = \frac{k_{12} \cdot C_{33}}{k_{13} - k_{11}} \quad (56)$$

$$C_{36} = \frac{k_{12} \cdot C_{34}}{k_{13} - k_{12}} \quad (57)$$

$$C_{37} = G_0 - C_{35} - C_{36} \quad (58)$$

$$C_{38} = TS_0 - TS_{RM} \cdot (1 - \alpha_{TS}) \quad (59)$$

$$C_{39} = TS_{RM} \cdot (1 - \alpha_{TS}) \quad (60)$$

$$C_{40} = \frac{k_{14} \cdot C_{38}}{k_{15} - k_{15}} \quad (61)$$

$$C_{41} = NVC_0 - C_{40} \quad (62)$$

Firstly, each temperature of pretreatment was modeled separately, obtaining the values of the susceptible fraction and the kinetic coefficients for each model and each temperature. Table 1 displays the values for the susceptible fraction of xylan, arabinan, acetyl groups, glucan and total solids, besides the kinetic coefficients k_1 to k_{15}, and the value R^2 which gives an idea of the goodness of the fit, for each temperature. Afterwards, the dependency of the kinetic coefficients with the temperature was modeled in accordance with the Arrhenius equation:

$$k_i = k_{i0} \cdot exp\left(-\frac{Ea}{R \cdot T}\right) \quad (63)$$

where k_i represents the kinetic coefficient (measured in min^{-1}), k_{i0} represents the pre-exponential factor (measured in min^{-1}), Ea represents the activation energy (measured in kJ/mol), R represents the ideal gas constant with a value of 8.314 J/(mol·K) and, T the absolute temperature (measured in K).

The fitting results of the kinetic coefficients to the equation (63) are displayed in table 2. Overall, the fitting of the different fractions was satisfactory. From the data analysis can be perceived that the values for the susceptible fraction show not too much variation regardless of the temperature used in the pretreatment, and α_{Arn} was very close to the unit.

A second strategy consisted on modeling all the temperatures jointly. To that end, it was assumed that the values of the susceptible fractions are constant, which was reasonable due to their little variation, and also the value of α_{Arn} was 1, which means that all the arabinan was susceptible. This was in accordance with what was observed in the modeling of each temperature separately and was correlated with the fact that the monomers of arabinose are always in the form of a side chain, favoring their hydrolysis. This second strategy was consequent with the well-known effect of the temperature over the kinetic coefficients, and would allow to lessen a lot the parameters needed for the fitting.

Fig. 2b shows the algorithm design for the calculation of the kinetic parameters of xylan and arabinan (algorithms for acetyl groups, glucan and total solids are simpler version of this one). The values of the susceptible fractions (Table 1), pre-exponential factors and activation energies (Table 2) obtained from the fitting of each temperature separately were set as initial values for the algorithm. The results from this fitting are presented in Table 3, and the comparison of the experimental and calculated for pentoses (xylan and arabinan), acetyl groups, glucan and total solid are shown in Figs. 3–6. The degree of concordance among the experimental and calculated values was very favorable as can be appreciated in the figures and in the values of R^2. It is worthy to mention that the first fitting strategy (using each temperature separately) needed 80 parameters, whereas the generalized fitting with all the temperatures jointly allowed to reduce the number of parameters to 34, without a greatly effect on the results.

Regarding each fraction, the xylan was the more affected by the process and its fitting for the residual xylan in the solid, xylooligosaccharides, xylose, furfural and decomposition products (although this species was calculated by difference) was very satisfactory. It is noteworthy the good degree of fitting in the conditions that lead to the maximum recovery of oligomers. Concerning the arabinan, the fitting results less precise for arabinooligosaccharides and arabinose due to the low content of arabinan in the Paulownia wood, which implies that the experimental error may affect proportionally more to this species. The acetyl groups were adequately modeled either for acetyl groups from the solid phase, acetyl groups linked to oligomers and acetic acid. On the subject of the residual glucan in the solid phase, it presents low values of fitting, however, this may be due to the low solubilization that take place. With regards to the fitting for the PW solubilization, the degree of fitting was also satisfactory.

Taking into account the lower number of parameters necessary to describe the pretreatment process in the second model proposed, only the data calculated using this model will be used for comparative purposes (see Table 3).

With regard to the reactive xylan (α_{Xn}), the value obtained was 0.888 g susceptible xylan/g xylan, which was similar to that obtained by Gullón et al. for vine shoots (0.881 g/g) (Gullón et al., 2017) and by Yañez and collaborators for *Acacia dealbata* (0.875 g/g) (Yáñez et al., 2009). The activation energy (Ea) for the hydrolysis of the xylan (124 kJ/mol) was considerably higher than the result reported by Rivas and colleagues (2016) in experiments with birch wood (65.6 kJ /mol) (Rivas et al., 2016) and it was slightly lower than for the autohydrolysis of vine shoots (156.9 kJ/mol) (Gullón et al., 2017). A comparison of Ea for the conversion of the high molecular weight XO to low molecular weight XO (128 kJ/mol) also indicated that the magnitude found here was much lower than that exhibited by vine shoots (225 kJ/mol) (Gullón et al., 2017). On the other hand, the Ea calculated for the conversion of XO_L to xylose was 119 kJ/mol, a value higher than that observed for the aforementioned feedstocks (78.3 kJ/mol for *Betula alba* and 94.2 for vine shoots) (Gullón et al., 2017; Rivas et al., 2016). In contrast, dos Santos Rocha et al. (2017) reported a value of Ea for the hydrolysis of XO to xylose in sugarcane straw of 1.85 times higher than that obtained in our research (dos Santos Rocha et al., 2017). The highest value of activation energy corresponded to the xylose dehydration to furfural (144 kJ/mol) and for the reaction of furfural to degradation products (171 kJ/mol). For the hydrolysis of the arabinosyl moieties, the activation energy values differ substantially to those observed for the previous feedstocks.

Concerning the glucan fraction susceptible to MHT (α_{Gn}), a value of 0.0550 g/g glucan was reached. This result was slightly lower than that observed in the hydrothermal pretreatment of rye straw (Gullón et al., 2010) and *Acacia dealbata* (Yáñez et al., 2009). According to Table 3, the

highest value for the activation energy was for the reaction of glucose to HMF (192 kJ/mol) and the lowest value was to the hydrolysis of GO to glucose (69.8 kJ/mol). In general, these results differed from those found by other authors. For instance, Gullón et al. (2010) reported a value of Ea for the transformation of the glucan to GO and glucose to HMF of 1.75 and 3 times lower, respectively, than that found in our work. In contrast, the reaction of GO to monomers for MHT of PW was substantially lower (69.2 kJ/mol) than that observed for rye straw (158 kJ/mol) (Gullón et al., 2010). In another study, dos Santos Rocha et al. reported values of Ea for the hydrolysis of the glucan to GO and GO to HMF significantly higher compared to those calculated here (dos Santos Rocha et al., 2017). The different results can be explained due to the different nature and compositions of the raw materials studied, besides the technology employed, either CHT or MHT.

The value calculated for the susceptible fraction of the acetyl groups ($\alpha_{AcG} = 0.933$ g susceptible acetyl groups/g acetyl groups, see Table 3) was comparable to those determined by Gullón et al. (2017) and Yañéz et al. (2009) (0.884 and 0.899 for vine shoots and *Acacia dealbata*, respectively). The Ea for the acetyl groups degradation reactions (108 and 111 kJ/mol) were analogous to the results observed for hardwoods such as *Acacia dealbata* (119 and 128 kJ/mol). In contrast, Gullón et al. (2017) reported much higher activation energy value for the transformation of acetyl groups into oligomers of vine shoots (274.4 kJ/mol) (Gullón et al., 2017; Yáñez et al., 2009).

Concerning the total solid, the susceptible fraction value was 0.335 g of susceptible total solid/g of raw PW, which was similar to the sum of the hemicellulosic fraction (21.9 g of hemicelluloses/100 g of raw PW, on dry basis) and the fraction of others (15.1 g of others/100 g of raw PW), which equal 37 g/100 g. This result agrees fairly well with the value calculated by Yáñez et al. (2009) for *Acacia dealbata* (0.329 g of susceptible total solid/g of oven-dried solid). On the other hand, the Ea value for the solubilization of the solid into NVC was 1.4 times lower than the one obtained by Yáñez et al. (2009) using *Acacia dealbata*. However, the activation energy value calculated for the transformation of the NVC into VC (137 kJ/mol) was in the order of magnitude to that reported in the same study (141 kJ/mol) (Yáñez et al., 2009).

4. Conclusions

MHT emerges as a viable technology for extracting hemicelluloses from PW. Under selected conditions (S_0 of 3.97–4.00), MHT allowed the solubilization of 80% of xylan into XO, while recovering about 95 and 100% of cellulose and lignin in pretreated PW, confirming the suitability of microwave-treatment as first step of a biorefinery. Besides, experimental data from MHT of PW were interpreted via kinetic models based on the parameters of Arrhenius equation. Overall, the two proposed models were satisfactory to fit the experimental data and may predict the behavior of MHT, providing information for scale-up process analysis and its further industrial development.

CRediT authorship contribution statement

Pablo G. del Río: Conceptualization, Formal analysis, Investigation, Methodology, Visualization, Writing - original draft, Writing - review & editing. **Beatriz Gullón:** Validation, Writing - review & editing. **Aloia Romaní:** Validation, Writing - review & editing. **Gil Garrote:** Conceptualization, Formal analysis, Funding acquisition, Supervision, Validation, Writing - review & editing.

Declaration of Competing Interest

The authors declare that they have no known competing financial interests or personal relationships that could have appeared to influence the work reported in this paper.

Acknowledgements

Authors are grateful to the University of Vigo and CISUG for the financial support of Open Access publication, to MINECO (Spain) for the financial support of this work in the framework of the projects "Cutting-edge strategies for a sustainable biorefinery based on valorization of invasive species" with reference PID2019-110031RB-I00 and, "Multi-stage projects for the integral benefit of macroalgae and vegetable biomass" with reference CTM2015-68503-R, and to Consellería de Cultura, Educación e Ordenación Universitaria (Xunta de Galicia) through the contract ED431C 2017/62-GRC to Competitive Reference Group BV1, programs partially funded by FEDER. Pablo G. del Río and Beatriz Gullón would like to express their gratitude to the Ministry of Science, Innovation and Universities of Spain for his FPU research grant (FPU16/04077) and her RYC grant (Grant reference RYC2018-026177-I), respectively.

Appendix A. Supplementary data

Supplementary data to this article can be found online at https://doi.org/10.1016/j.biortech.2021.125535.

References

Aguilar-Reynosa, A., Romaní, A., Rodríguez-Jasso, R.M., Aguilar, C.N., Garrote, G., Ruiz, H.A., 2017a. Microwave heating processing as alternative of pretreatment in second-generation biorefinery: An overview. Energy Convers. Manag. 136, 50–65. https://doi.org/10.1016/j.enconman.2017.01.004.

Aguilar-Reynosa, A., Romaní, A., Rodríguez-Jasso, R.M., Aguilar, C.N., Garrote, G., Ruiz, H.A., 2017b. Comparison of microwave and conduction-convection heating autohydrolysis pretreatment for bioethanol production. Bioresour. Technol. 243, 273–283. https://doi.org/10.1016/j.biortech.2017.06.096.

Branco, P.C., Dionísio, A.M., Torrado, I., Carvalheiro, F., Castilho, P.C., Duarte, L.C., 2015. Autohydrolysis of *Annona cherimola* Mill. seeds: Optimization, modeling and products characterization. Biochem. Eng. J. 104, 2–9. https://doi.org/10.1016/j.bej.2015.06.006.

Cao, F., Xia, S., Yang, X., Wang, C., Wang, Q.i., Cui, C., Zheng, A., 2020. Lowering the pyrolysis temperature of lignocellulosic biomass by H_2SO_4 loading for enhancing the production of platform chemicals. Chem. Eng. J. 385, 123809. https://doi.org/10.1016/j.cej.2019.123809.

Caparrós, S., Garrote, G., Ariza, J., López, F., 2006. Autohydrolysis of *Arundo donax* L., a kinetic assessment. Ind. Eng. Chem. Res. 45 (26), 8909–8920. https://doi.org/10.1021/ie061166x.

Carvalheiro, F., Garrote, G., Parajó, J.C., Pereira, H., Gírio, F.M., 2005. Kinetic modeling of brewery's spent grain autohydrolysis. Biotechnol. Prog. 21, 233–243. https://doi.org/10.1021/bp049764z.

Chandel, A.K., Garlapati, V.K., Jeevan Kumar, S.P., Hans, M., Singh, A.K., Kumar, S., 2020. The role of renewable chemicals and biofuels in building a bioeconomy. Biofuels. Bioprod. Biorefining 14 (4), 830–844. https://doi.org/10.1002/bbb.v14.410.1002/bbb.2104.

Chin, S.X., Chia, C.H., Fang, Z., Zakaria, S., Li, X.K., Zhang, F., 2014. A kinetic study on acid hydrolysis of oil palm empty fruit bunch fibers using a microwave reactor system. Energy and Fuels 28 (4), 2589–2597. https://doi.org/10.1021/ef402468z.

Conner, A., Lorenz, L., 1986. Kinetic modeling of hardwood prehydrolysis. III: Water and dilute acetic acid prehydrolysis of southern red oak. Wood fiber Sci. 18, 248–263.

Cunha, J.T., Soares, P.O., Romaní, A., Thevelein, J.M., Domingues, L., 2019. Xylose fermentation efficiency of industrial *Saccharomyces cerevisiae* yeast with separate or combined xylose reductase/xylitol dehydrogenase and xylose isomerase pathways. Biotechnol. Biofuels 12, 1–14. https://doi.org/10.1186/s13068-019-1360-8.

da Silva Lacerda, V., López-Sotelo, J.B., Correa-Guimarães, A., Hernández-Navarro, S., Sánchez-Bascones, M., Navas-Gracia, L.M., Martín-Ramos, P., Pérez-Lebeña, E., Martín-Gil, J., 2015. A kinetic study on microwave-assisted conversion of cellulose and lignocellulosic waste into hydroxymethylfurfural/furfural. Bioresour. Technol. 180, 88–96. https://doi.org/10.1016/j.biortech.2014.12.089.

Dávila, I., Gullón, B., Alonso, J.L., Labidi, J., Gullón, P., 2019. Vine shoots as new source for the manufacture of prebiotic oligosaccharides. Carbohydr. Polym. 207, 34–43. https://doi.org/10.1016/j.carbpol.2018.11.065.

del Río, P.G., Domínguez, E., Domínguez, V.D., Romaní, A., Domingues, L., Garrote, G., 2019. Third generation bioethanol from invasive macroalgae *Sargassum muticum* using autohydrolysis pretreatment as first step of a biorefinery. Renew. Energy 141, 728–735. https://doi.org/10.1016/j.renene.2019.03.083.

del Río, P.G., Domínguez, V.D., Domínguez, E., Gullón, P., Gullón, B., Garrote, G., Romaní, A., 2020a. Comparative study of biorefinery processes for the valorization of fast-growing Paulownia wood. Bioresour. Technol. 314, 123722. https://doi.org/10.1016/j.biortech.2020.123722.

del Río, P.G., Gomes-Dias, J.S., Rocha, C.M.R., Romaní, A., Garrote, G., Domingues, L., 2020b. Recent trends on seaweed fractionation for liquid biofuels production. Bioresour. Technol. 299, 122613. https://doi.org/10.1016/j.biortech.2019.122613.

del Río, P.G., Gullón, P., Rebelo, F.R., Romaní, A., Garrote, G., Gullón, B., 2020c. A whole-slurry fermentation approach to high-solid loading for bioethanol production from corn stover. Agronomy 10, 1790. https://doi.org/10.3390/agronomy10111790.

Díaz-Fernández, D., Aguiar, T.Q., Martín, V.I., Romaní, A., Silva, R., Domingues, L., Revuelta, J.L., Jiménez, A., 2019. Microbial lipids from industrial wastes using xylose-utilizing *Ashbya gossypii* strains. Bioresour. Technol. 293, 122054. https://doi.org/10.1016/j.biortech.2019.122054.

Domínguez, E., del Río, P.G., Romaní, A., Garrote, G., Domingues, L., 2021. Hemicellulosic bioethanol production from fast-growing Paulownia biomass. Processes 9, 1–15. https://doi.org/10.3390/pr9010173.

Domínguez, E., Nóvoa, T., del Río, P.G., Garrote, G., Romaní, A., 2020. Sequential two-stage autohydrolysis biorefinery for the production of bioethanol from fast-growing Paulownia biomass. Energy Convers. Manag. 226, 113517. https://doi.org/10.1016/j.enconman.2020.113517.

Domínguez, E., Romaní, A., Domingues, L., Garrote, G., 2017. Evaluation of strategies for second generation bioethanol production from fast growing biomass Paulownia within a biorefinery scheme. Appl. Energy 187, 777–789. https://doi.org/10.1016/j.apenergy.2016.11.114.

dos Santos Rocha, M.S.R., Pratto, B., de Sousa, R., Almeida, R.M.R.G., Cruz, A.J.G.d., 2017. A kinetic model for hydrothermal pretreatment of sugarcane straw. Bioresour. Technol. 228, 176–185. https://doi.org/10.1016/j.biortech.2016.12.087.

Ershova, O., Kanervo, J., Hellsten, S., Sixta, H., 2015. The role of xylulose as an intermediate in xylose conversion to furfural: insights via experiments and kinetic modelling. RSC Adv. 5 (82), 66727–66737. https://doi.org/10.1039/C5RA10855A.

Fernandes Antunes, F.A., Chandel, A.K., Terán-Hilares, R., Ingle, A.P., Rai, M., dos Santos Milessi, T.S., Silvério da Silva, S., dos Santos, J.C., 2019. Overcoming challenges in lignocellulosic biomass pretreatment for second-generation (2G) sugar production: emerging role of nano, biotechnological and promising approaches. 3. Biotech 9, 230. https://doi.org/10.1007/s13205-019-1761-1.

Ferreira, J.A., Taherzadeh, M.J., 2020. Improving the economy of lignocellulose-based biorefineries with organosolv pretreatment. Bioresour. Technol. 299, 122695. https://doi.org/10.1016/j.biortech.2019.122695.

Garrote, G., Domínguez, H., Parajó, J.C., 2004. Production of substituted oligosaccharides by hydrolytic processing of barley husks. Ind. Eng. Chem. Res. 43 (7), 1608–1614. https://doi.org/10.1021/ie0342762.

González-García, S., Argiz, L., Míguez, P., Gullón, B., 2018. Exploring the production of bio-succinic acid from apple pomace using an environmental approach. Chem. Eng. J. 350, 982–991. https://doi.org/10.1016/j.cej.2018.06.052.

Gullón, B., Eibes, G., Dávila, I., Vila, C., Labidi, J., Gullón, P., 2017. Valorization of vine shoots based on the autohydrolysis fractionation optimized by a kinetic approach. Ind. Eng. Chem. Res. 56 (48), 14164–14171. https://doi.org/10.1021/acs.iecr.7b02833.

Gullón, B., Yáñez, R., Alonso, J.L., Parajó, J.C., 2010. Production of oligosaccharides and sugars from rye straw: A kinetic approach. Bioresour. Technol. 101 (17), 6676–6684. https://doi.org/10.1016/j.biortech.2010.03.080.

Gullón, P., Gullón, B., Astray, G., Carpena, M., Fraga-Corral, M., Prieto, M.A., Simal-Gandara, J., 2020. Valorization of by-products from olive oil industry and added-value applications for innovative functional foods. Food Res. Int. 137, 109683. https://doi.org/10.1016/j.foodres.2020.109683.

Gullón, P., Romaní, A., Vila, C., Garrote, G., Parajó, J.C., 2012. Potential of hydrothermal treatments in lignocellulose biorefineries. Biofuels. Bioprod. Biorefining 6, 219–232. https://doi.org/10.1002/bbb.

Ingle, A.P., Philippini, R.R., de Souza Melo, Y.C., da Silva, S.S., 2020. Acid-functionalized magnetic nanocatalysts mediated pretreatment of sugarcane straw: an eco-friendly and cost-effective approach. Cellulose 27 (12), 7067–7078. https://doi.org/10.1007/s10570-020-03262-y.

Jorissen, T., Oraby, A., Recke, G., Zibek, S., 2020. A systematic analysis of economic evaluation studies of second-generation biorefineries providing chemicals by applying biotechnological processes. Biofuels. Bioprod. Biorefining 14 (5), 1028–1045. https://doi.org/10.1002/bbb.v14.510.1002/bbb.2102.

Kabel, M.A., Carvalheiro, F., Garrote, G., Avgerinos, E., Koukios, E., Parajó, J.C., Gírio, F. M., Schols, H.A., Voragen, A.G.J., 2002. Hydrothermally treated xylan rich by-products yield different classes of xylo-oligosaccharides. Carbohydr. Polym. 50, 47–56. https://doi.org/10.1016/S0144-8617(02)00045-0.

Lloyd, T., Wyman, C.E., 2003. Application of a depolymerization model for predicting thermochemical hydrolysis of hemicellulose. Appl. Biochem. Biotechnol. 105 (1-3), 53–68. https://doi.org/10.1385/ABAB:105:1-3:53.

López-Linares, J.C., García-Cubero, M.T., Lucas, S., González-Benito, G., Coca, M., 2019. Microwave assisted hydrothermal as greener pretreatment of brewer's spent grains for biobutanol production. Chem. Eng. J. 368, 1045–1055. https://doi.org/10.1016/j.cej.2019.03.032.

Meng, L.Y., Wang, B., Ma, M.G., Lin, K.L., 2016. The progress of microwave-assisted hydrothermal method in the synthesis of functional nanomaterials. Mater. Today Chem. 1–2, 63–83. https://doi.org/10.1016/j.mtchem.2016.11.003.

Oleszek, M., Kowalska, I., Oleszek, W., 2019. Phytochemicals in bioenergy crops, Phytochemistry Reviews. Springer Netherlands. https://doi.org/10.1007/s11101-019-09639-7.

Rivas, S., Vila, C., Santos, V., Parajó, J.C., 2016. Furfural production from birch hemicelluloses by two-step processing: A potential technology for biorefineries. Holzforschung 70, 901–910. https://doi.org/10.1515/hf-2015-0255.

Romaní, A., Morais, E.S., Soares, P.O., Freire, M.G., Freire, C.S.R., Silvestre, A.J.D., Domingues, L., 2020. Aqueous solutions of deep eutectic systems as reaction media for the saccharification and fermentation of hardwood xylan into xylitol. Bioresour. Technol. 311, 123524. https://doi.org/10.1016/j.biortech.2020.123524.

Sanahuja-Parejo, O., Veses, A., Navarro, M.V., López, J.M., Murillo, R., Callén, M.S., García, T., 2019. Drop-in biofuels from the co-pyrolysis of grape seeds and polystyrene. Chem. Eng. J. 377, 120246. https://doi.org/10.1016/j.cej.2018.10.183.

Sannigrahi, P., Kim, D.H., Jung, S., Ragauskas, A., 2011. Pseudo-lignin and pretreatment chemistry. Energy Environ. Sci. 4 (4), 1306–1310. https://doi.org/10.1039/C0EE00378F.

Santucci, B.S., Maziero, P., Rabelo, S.C., Curvelo, A.A.S., Pimenta, M.T.B., 2015. Autohydrolysis of hemicelluloses from sugarcane bagasse during hydrothermal pretreatment: A kinetic assessment. Bioenergy Res. 8 (4), 1778–1787. https://doi.org/10.1007/s12155-015-9632-z.

Sluiter, A., Hames, B., Hyman, D., Payne, C., Ruiz, R., Scarlata, C., Sluiter, J., Templeton, D., Wolfe, J., 2008a. Determination of total solids in biomass and total dissolved solids in liquid process samples. Laboratory Analytical Procedure (LAP). Natl. Renew. Energy Lab. 1, 1–6 https://doi.org/NREL/TP-510-42621.

Sluiter, A., Hames, B., Ruiz, R., Scarlata, C., Sluiter, J., Templeton, D., 2008b. Determination of ash in biomass. Laboratory Analytical Procedure (LAP). Natl. Renew. Energy Lab. 1, 1–5 https://doi.org/NREL/TP-510-42619.

Sluiter, A., Hames, B., Ruiz, R., Scarlata, C., Sluiter, J., Templeton, D., Crocker, D., 2008c. Determination of structural carbohydrates and lignin in biomass. Laboratory Analytical Procedure (LAP). Natl. Renew. Energy Lab. 1, 1–15 https://doi.org/NREL/TP-510-42618.

Sluiter, A., Ruiz, R., Scarlata, C., Sluiter, J., Templeton, D., 2008d. Determination of Extractives in Biomass. Laboratory Analytical Procedure (LAP). Natl. Renew. Energy Lab. 1, 1–9. https://doi.org/10.1016/j.rmr.2016.02.006.

Sweygers, N., Depuydt, D.E.C., Van Vuure, A.W., Degrève, J., Potters, G., Dewil, R., Appels, L., 2020. Simultaneous production of 5-hydroxymethylfurfural and furfural from bamboo (*Phyllostachys nigra* "Boryana") in a biphasic reaction system. Chem. Eng. J. 386, 123957. https://doi.org/10.1016/j.cej.2019.123957.

Vargas, F., Domínguez, E., Vila, C., Rodríguez, A., Garrote, G., 2016. Biorefinery scheme for residual biomass using autohydrolysis and organosolv stages for oligomers and bioethanol production. Energy and Fuels 30 (10), 8236–8245. https://doi.org/10.1021/acs.energyfuels.6b00277.

Yáñez, R., Romaní, A., Garrote, G., Alonso, J.L., Parajó, J.C., 2009. Processing of *Acacia dealbata* in aqueous media: First step of a wood biorefinery. Ind. Eng. Chem. Res. 48 (14), 6618–6626. https://doi.org/10.1021/ie900233x.

Zhu, Y.-J., Chen, F., 2014. Microwave-assisted preparation of inorganic nanostructures in liquid phase. Chem. Rev. 114 (12), 6462–6555. https://doi.org/10.1021/cr400366s.